On Study of Lunar Microwave Brightness Temperature Spectrum based on Satellite Observations

Hu(Tiger) Yang
ESSIC, University of Maryland
huyang@umd.edu
Nov.18, 2020

Outline

- Introduction of ATMS instrument
- Theoretical model for lunar microwave emission
- Microwave brightness temperature spectrum from NOAA-20 ATMS 2-D Moon scan observations
- Phase angle dependent feature derived from drifting orbit of NOAA-18 AMSU
- Conclusion and Future work

ATMS Instrument Description

Simplified ATMS Block Diagram (Ed Kim et al., JGR 2014)

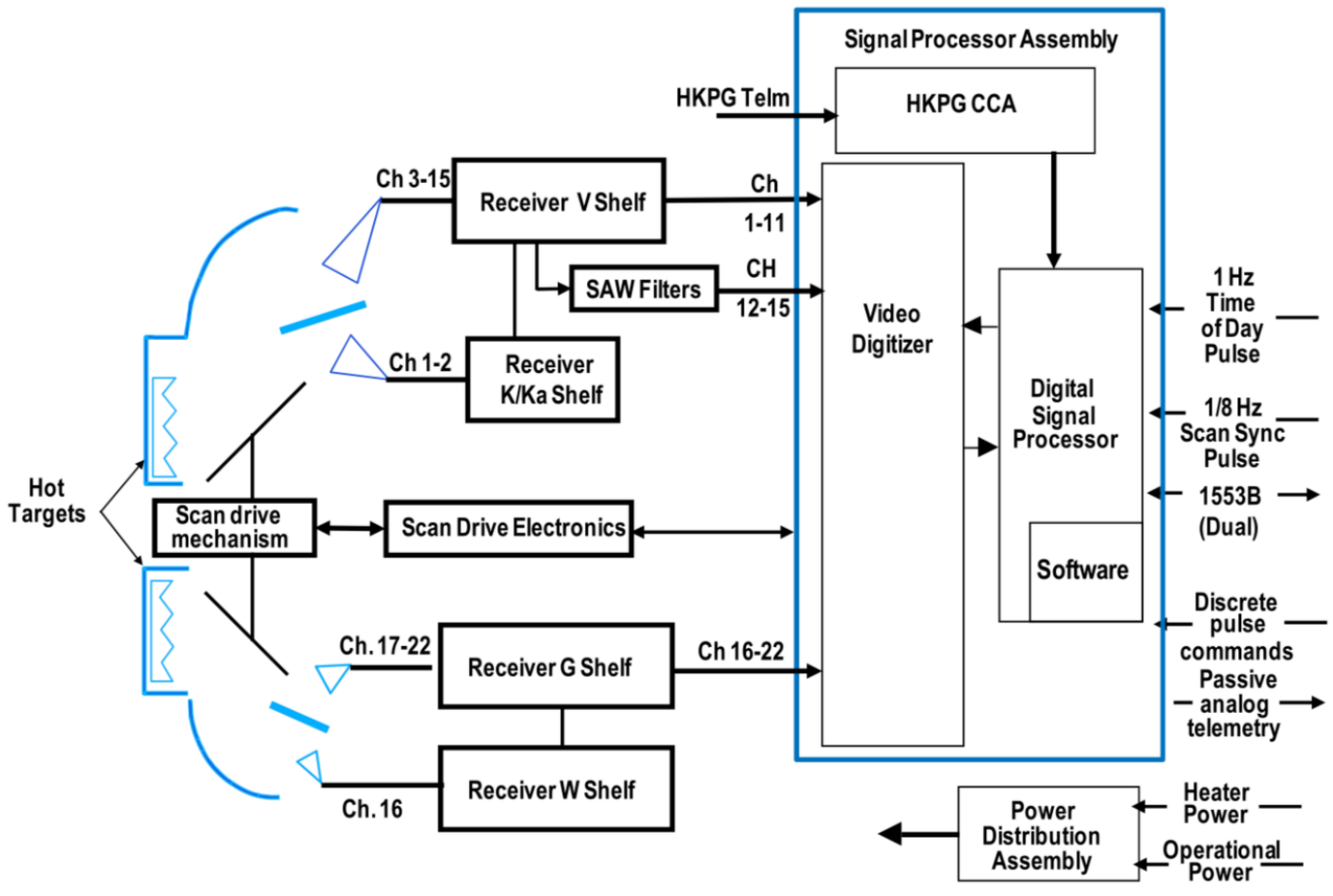

ATMS Spectrometric and Radiometric Specification

Ch	RF path			Center frequency [MHz]		Bandwidth [MHz]		NEDT [K]	Pol	Beamwidth [°]
	Ant	Feed	Rcvr	Value	Stab	Req	True	Req		Req
1	A	1	a	23800	<10	<270	1x270	0.5	V	5.2
2	A	1	b	31400	<10	<180	1x180	0.6	V	5.2
3	A	2	c	50300	<10	<180	1x180	0.7	H	2.2
4	A	2	c	51760	< 5	<400	1x400	0.5	H	2.2
5	A	2	c	52800	< 5	<400	1x400	0.5	H	2.2
6	A	2	c	53596±115	< 5	170	2x170	0.5	H	2.2
7	A	2	c	54400	< 5	400	1x400	0.5	H	2.2
8	A	2	c	54940	<10	400	1x400	0.5	H	2.2
9	A	2	c	55500	<10	330	1x330	0.5	H	2.2
10	A	2	d_1	57290.344 [f_0]	<0.5	330	2x155	0.75	H	2.2
11	A	2	d_1	f_0±217	<0.5	78	2x 78	1.0	H	2.2
12	A	2	d_2	f_0±322.2±48	<1.2	36	4x 36	1.0	H	2.2
13	A	2	d_2	f_0±322.±22	<1.6	16	4x 16	1.5	H	2.2
14	A	2	d_2	f_0±322.±10	<0.5	8	4x 8	2.2	H	2.2
15	A	2	d_2	f_0±322.±4.5	<0.5	3	4x 3	3.6	H	2.2
16	B	3	e	88200	<200	2000	1x2000	0.3	V	2.2
17	B	4	f	165500	<200	3000	2x1150	0.6	H	1.1
18	B	4	g	183310±7000	<30	2000	2x2000	0.8	H	1.1
19	B	4	g	183310±4500	<30	2000	2x2000	0.8	H	1.1
20	B	4	g	183310±3000	<30	1000	2x1000	0.8	H	1.1
21	B	4	g	183310±1800	<30	1000	2x1000	0.8	H	1.1
22	B	4	g	183310±1000	<30	500	2x 500	0.9	H	1.1

ATMS Instrument Calibration Error Budget Analysis

The ATMS radiometric calibration for antenna brightness temperature is derived as

$$R = R_c + (R_w - R_c)\left(\frac{C_s - \overline{C_c}}{\overline{C_w} - \overline{C_c}}\right) + Q$$

Considering the system noise and gain drift errors, the error model for ATMS calibration can be derived as:

$$\Delta R = x\Delta R_w + (1-x)\Delta R_c + 4Q^{\max}(x - x^2) \pm RMSError$$

ATMS Scan Geometry

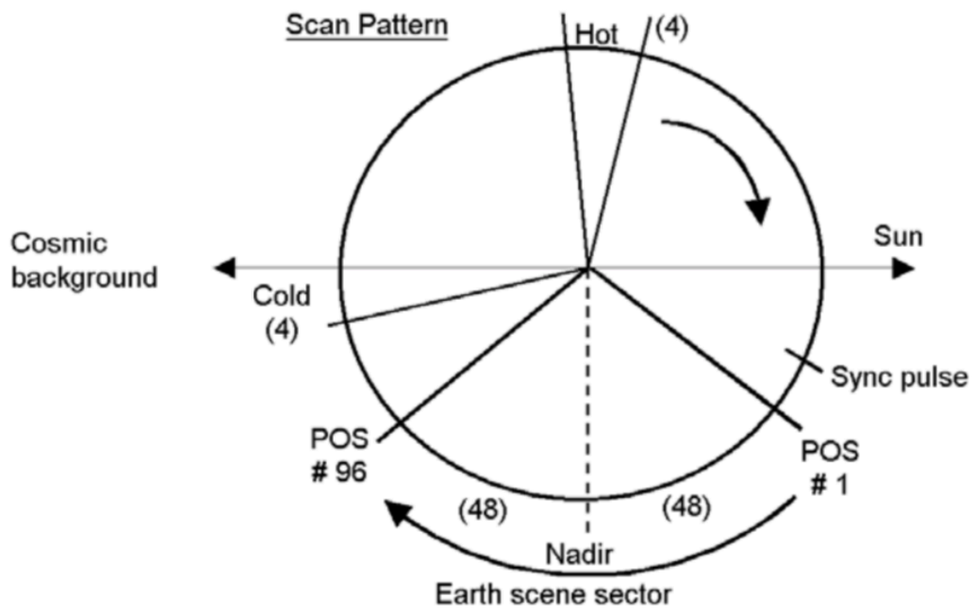

ΔR_w Error in determine warm target radiance

ΔR_c Error in determine cold target radiance

$Q^{\max}$ Maximum nonlinearity

$RMSError$ System noise and gain drift errors

Error Budget Results for in-flight SNPP/J1 ATMS

Laboratory microwave calibration standard is needed to make warm load become SI-traceable on-orbit calibration reference

Channel	Warm Target Emissivity	Coupling Loss	Cold-Target Contamination-Earth RMS Error	Peak Non-linearity SNPP ATMS				Peak Non-linearity J1 ATMS			
				RC1	RC2	RC5	RC6	RC1	RC2	RC5	RC6
1	0.999999	0.1205	0.117	0.219	0.278	0.265	0.264	0.59	0.58	0.55	0.55
2	0.999998	0.1205	0.192	0.022	0.093	0.097	0.074	0.64	0.61	0.64	0.63
3	0.999998	0.1154	0.092	0.113	0.172	0.211	0.169	0.01	-0.01	0.00	0.03
4	1.000000	0.1154	0.084	0.212	0.266	0.221	0.239	-0.11	-0.09	-0.11	-0.12
5	1.000000	0.1154	0.092	0.171	0.256	0.242	0.222	-0.06	-0.04	-0.05	-0.07
6	0.999997	0.1154	0.084	0.055	0.117	0.148	0.143	-0.11	-0.09	-0.09	-0.08
7	0.999996	0.1154	0.092	0.061	0.098	0.101	0.093	0.15	0.16	0.15	0.14
8	0.999995	0.1154	0.109	0.164	0.250	0.237	0.222	0.22	0.23	0.24	0.22
9	0.999996	0.1154	0.100	-0.061	0.003	0.020	0.019	0.22	0.21	0.22	0.21
10	0.999997	0.1154	0.084	0.155	0.204	0.156	0.138	0.58	0.60	0.57	0.62
11	0.999997	0.1154	0.084	0.230	0.219	0.282	0.253	0.65	0.59	0.57	0.57
12	0.999997	0.1154	0.084	0.161	0.266	0.214	0.163	0.68	0.76	0.73	0.62
13	0.999997	0.1154	0.084	0.134	0.233	0.215	0.115	0.79	0.80	0.77	0.76
14	0.999997	0.1154	0.084	-0.130	-0.113	-0.062	0.010	0.56	0.69	0.54	0.68
15	0.999997	0.1154	0.084	0.192	0.292	0.098	0.219	0.59	0.72	0.68	0.56
16	0.999999	0.0760	0.326	0.240	0.296	0.309	0.327	0.16	0.17	0.15	0.12
17	0.999983	0.0551	0.050	0.304	0.390	0.384	0.397	0.46	0.44	0.41	0.42
18	0.999964	0.0551	0.067	0.227	0.289	0.277	0.308	0.20	0.20	0.21	0.19
19	0.999964	0.0551	0.067	0.270	0.308	0.350	0.351	0.18	0.17	0.18	0.18
20	0.999964	0.0551	0.067	0.324	0.302	0.338	0.337	0.15	0.18	0.19	0.16
21	0.999964	0.0551	0.067	0.246	0.282	0.287	0.357	0.14	0.20	0.24	0.14
22	0.999979	0.0551	0.025	0.305	0.295	0.349	0.343	0.38	0.34	0.31	0.35

Peer Review Publications for ATMS Cal/Val Sciences

Calibration Algorithm

- Edward Kim Cheng-Hsuan J. Lyu Kent Anderson R. Vincent Leslie William J. Blackwell, 2014, "S-NPP ATMS instrument prelaunch and on-orbit performance evaluation"JGR, 2014 https://doi.org/10.1002/2013JD020483
- Fuzhong Weng, Xiaolei Zou, Ninghai Sun, Hu Yang, Xiang Wang, Lin Lin, Miao Tian, and Kent Anderson, 2013, "Calibration of Suomi National Polar-Orbiting Partnership (NPP) Advanced Technology Microwave Sounder (ATMS) ", Journal of Geophysical Research, Vol.118, No.19, PP. 11,187~11,200
- Weng, F. and Yang, H., 2016. Validation of ATMS calibration accuracy using Suomi NPP pitch maneuver observations. Remote Sensing, 8(4), p.332

Antenna Correction

- Hu Yang and Fuzhong Weng, Kent Anderson, 2016, "Estimation of ATMS Antenna Emission from Cold Space Observations", , IEEE Geoscience and Remote sensing, 10.1109/TGRS.2016.2542526"
- Fuzhong Weng, Hu Yang, Xiaolei Zou,2013, "On Convertibility From Antenna to Sensor Brightness Temperature for ATMS", IEEE Geoscience and Remote sensing Letters, 2012, Vol.99, pp 1-5

Remapping SDR

- Hu Yang and Xiaolei Zou, X, 2014. Optimal ATMS remapping algorithm for climate research. Geoscience and Remote Sensing, IEEE Transactions on Geoscience and Remote Sensing, 52(11), 7290-7296.

Lunar Contamination Correction

- Hu Yang and Fuzhong Weng, 2016, "On-Orbit ATMS Lunar Contamination Corrections", IEEE Transactions on Geoscience and Remote Sensing, Vol. 54 Issue: 4, page(s): 1-7

Vicarious calibration and Long-term stability Monitoring

- Hu Yang, Jun Zhou, Ninghai Sun, Kent Anderson, Quanhua Liu, Ed Kim, 2018, "Developing vicarious calibration for microwave sounding instruments using lunar radiation", IEEE Transactions on Geoscience and Remote Sensing, Vol.99, PP.1-11

Geolocation correction and Validation

- Jun Zhou and Hu Yang, 2019, "On Study of Two-Dimensional Lunar Scan for Advanced Technology Microwave Sounder Geometric Calibration", Atmospheric Measurement Technique, https://doi.org/10.5194/amt-2019-177
- Jun Zhou, Hu Yang and Kent Anderson, 2019, "SNPP ATMS On-Orbit Geolocation Error Evaluation and Correction Algorithm", IEEE Transactions on Geoscience and Remote Sensing 57 (6), 3802-3812

Observation Model for Antenna Temperature of the Moon's Disk

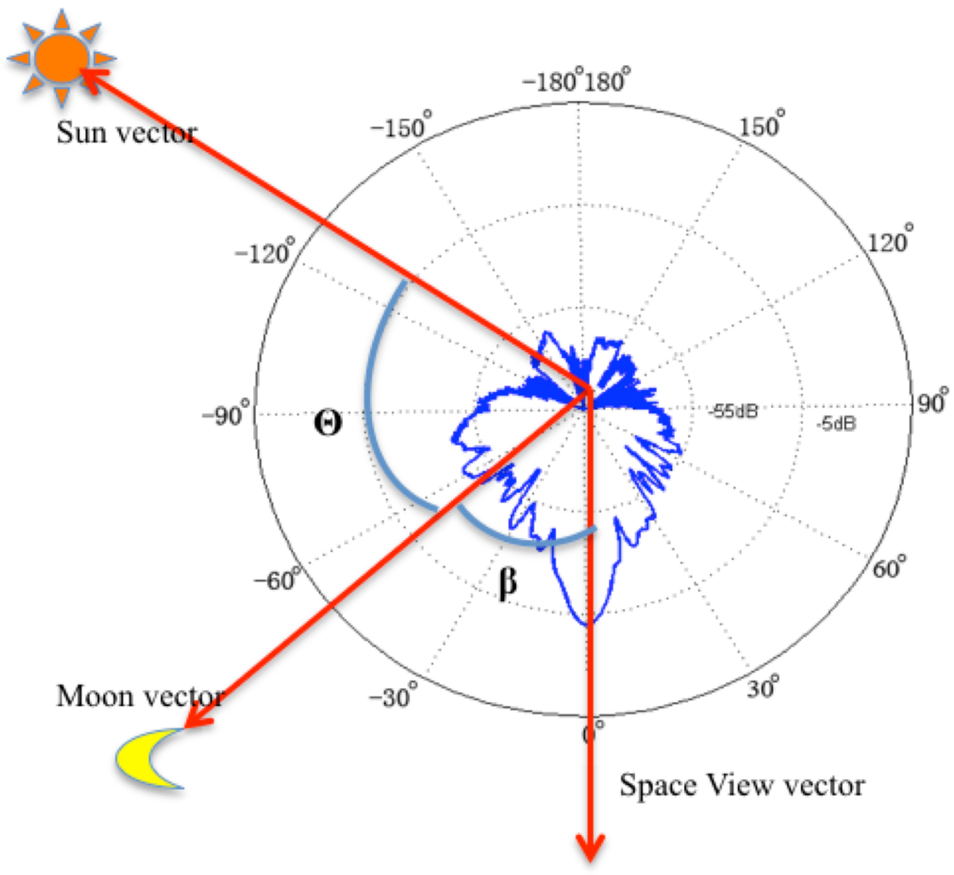

When the Moon appears in satellite observation field of view (FOV), the effective microwave brightness temperature of moon's disk, can be expressed as function of antenna response function G_{ant}, normalized solid angle of the moon Ω_{moon}, and average brightness temperature of the moon's disk :

$$TB_{moon}^{eff} = \Omega_{moon} \cdot G_{ant} \cdot TB_{moon}^{disk}$$

Assuming the azimuthal asymmetry is insignificant, the antenna response within the mean beam range can then be accurately simulated by one dimension Gaussian function:

$$G_{ant}(\beta') = e^{-(\beta' - \alpha_0)^2 / 2 \cdot \sigma^2}$$

where β is the separation angle between antenna boresight and Moon-in-View vector, α_0 is the beam pointing error angle. The normalized solid angle of moon is calculated as a solid angle of moon disk normalized by the beam solid angle, :

$$\Omega_{moon} = \frac{\pi\left(\frac{r_{moon}}{D_{moon}}\right)^2}{\Omega_A}$$

Beam solid angle can be calculated from ground measured antenna pattern data as:

$$\Omega_A = \iint_{4\pi} G(\theta, \phi) sin\theta \, d\theta \, d\varphi.$$

Two-Dimension Lunar Scan Observations from NOAA020 ATMS

The NOAA-20 satellite was successfully launched on 18 November 2017. On January 31, 2018, the spacecraft performed a pitch-over maneuver operation, during which the two-dimensional lunar scan observations were collected. Due to the orientation of NOAA-20 orbits, radiation from a full Moon disk with closely to 180 deg phase angle were collected when the Moon passing through the antenna beam

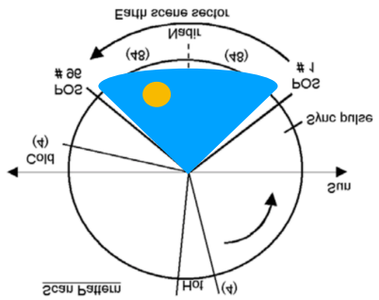

- The observed raw data counts were transferred to brightness temperature by using the calibration equation with the warm load and cold space observations.
- Further corrections for warm bias, earth side lobe contamination, as well as the reflector emission contamination are needed.
- To derive the pure lunar signal, the cosmic background radiation is subtracted from the calibrated brightness temperature.

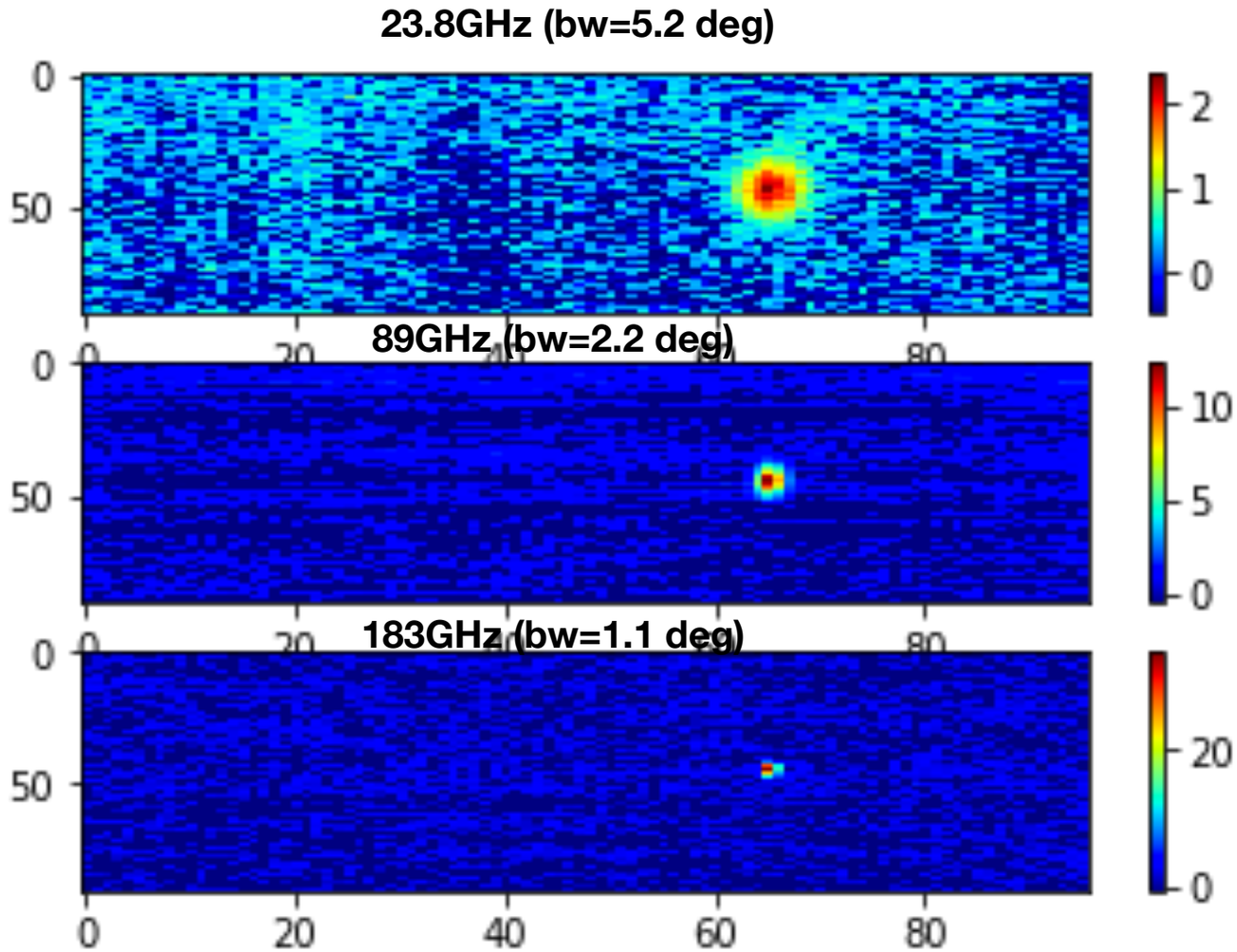

2-D Geometry Model for Microwave Moon Observations

Dynamic Antenna Coordinate System for Lunar Scan

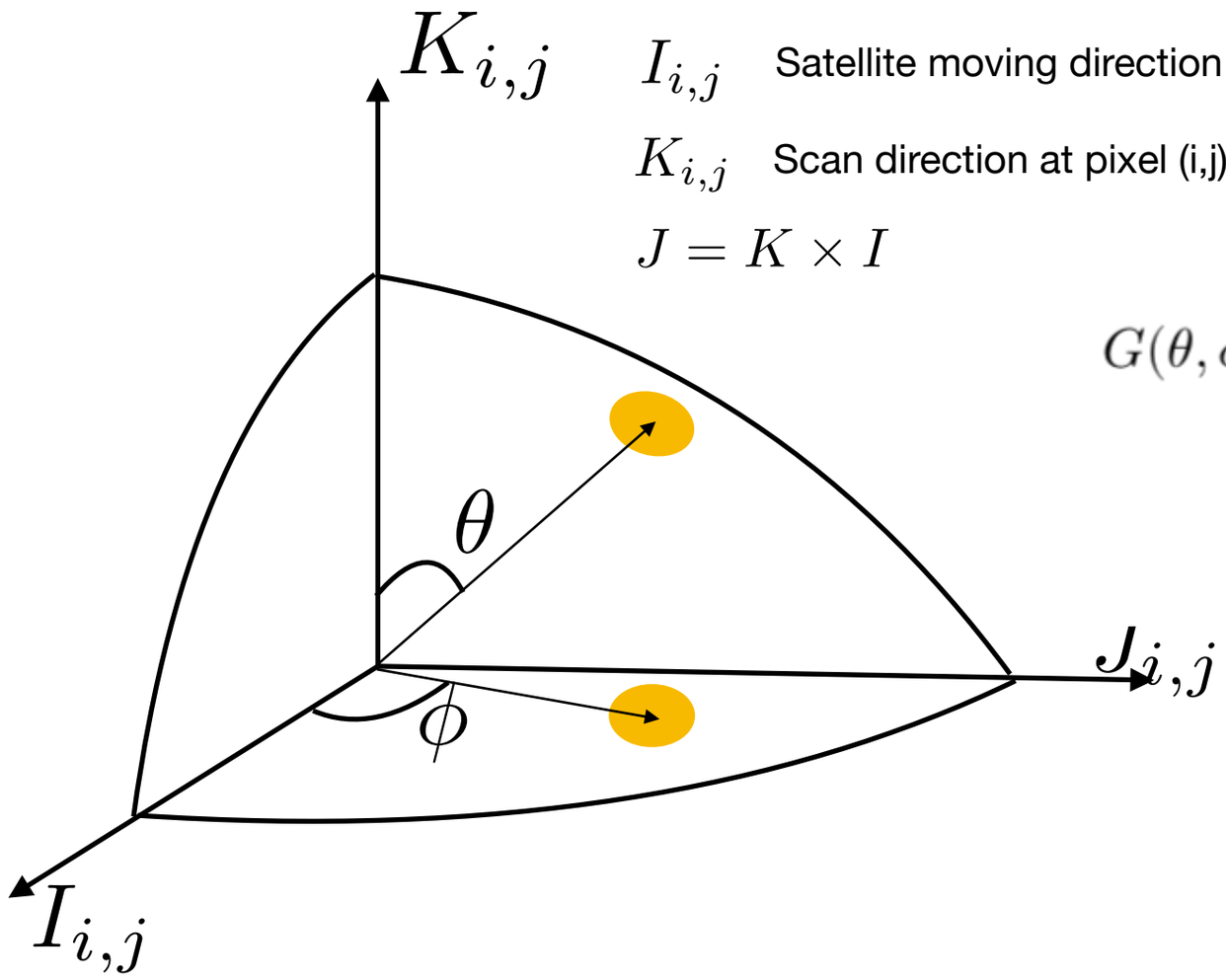

$I_{i,j}$ Satellite moving direction at pixel (i,j)

$K_{i,j}$ Scan direction at pixel (i,j)

$J = K \times I$

$$G(\theta,\phi) = \exp -[\frac{(x-x_0)^2}{2\sigma_x^2} + \frac{(y-y_0)^2}{2\sigma_y^2}]$$

$$x = sin\theta \cdot cos\phi$$

$$y = sin\theta \cdot sin\phi$$

$$Ta_{moon}(\theta_{ifov},\phi_{ifov}) = \frac{Tb_{moon}^{Disk}\Omega_{moon}}{\Omega_p} G(\theta_{ifov},\phi_{ifov})$$

$Ta_{moon}(\theta_{ifov},\phi_{ifov})$ observed antenna temperature of Moon

Tb_{moon}^{Disk} Disk integrated brightness temperature of lunar surface

Ω_{moon} Solid angle of Moon at observed antenna beam width

Ω_p Antenna solid angle

$G(\theta_{ifov},\phi_{ifov})$ Antenna response of lunar observations at specified scan position

Beam Pointing Error Corrections

*Zhou, J. and **Yang, H***., "A study of a two-dimensional scanned lunar image for Advanced Technology Microwave Sounder (ATMS) geometric calibration", Atmospheric Measurement Techniques, vol. 12, no. 9, pp. 4983–4992, 2019. doi:10.5194/amt-12-4983-2019.*

Considering the facts that the magnitude of antenna response is very sensitive to position of Moon's center in the Field of View of antenna beam on observing direction. Especially when lunar appears at the center of FOV, where the gradient of antenna response reaches its maximum. Therefore by comparing simulated antenna response of lunar scans with the observation truth, the displacement of beam center can be identified.

Given (ξ_r, ξ_p) are roll and pitch Euler angles error in ATMS geometric calibration, the optimum (ξ_r, ξ_p) value can be determined by finding the minima of the function below:

$$\sigma(\xi_r, \xi_p) = \frac{1}{N-1}\sqrt{\sum_{i=1}^{N}(G(\xi_r, \xi_p) - G_{obs})^2}$$

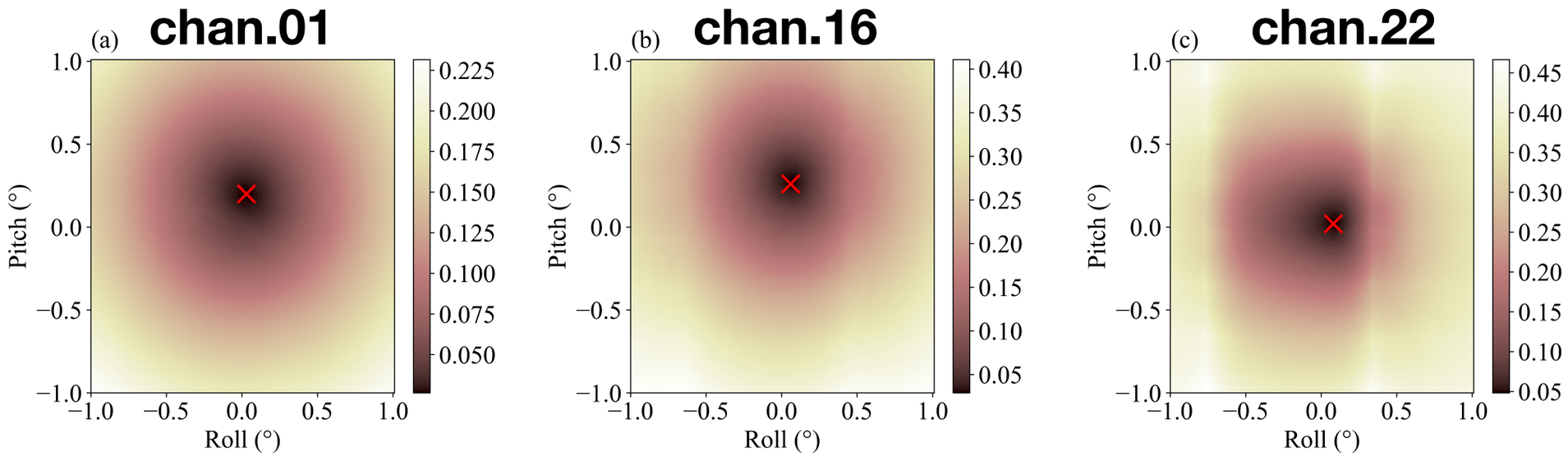

Retrieving of Lunar Microwave Brightness Temperature Spectrum

The calibrated antenna temperature of the Moon's disk of each data sample in a ATMS lunar scan, Ta_{moon}, is the radiance received from the Moon's disk integrated over a 18-ms sampling time along the moving path, which can be modeled as a function of the disk-integrated lunar microwave brightness temperature (Tb_{moon}^{Disk}), the antenna main beam solid angle (Ω_p), and the normalized antenna response (G) as follows:

$$Ta_{moon}(\theta_{ifov}, \phi_{ifov}) = Tb_{moon}^{Disk} \cdot \frac{G(\theta_{ifov}, \phi_{ifov})}{\Omega_P}.$$

For lunar observations at each scan position, the antenna response can be simulated as the solid-angle integration of the lunar disk over the instrument integration time along the moving path of the Moon on the surface of the normalized antenna pattern, expressed as follows:

$$G(\theta_{ifov}, \phi_{ifov}) = \Omega_{moon}^{ifov}$$
$$= \frac{1}{\mathcal{L}} \int_{\frac{-\tau}{2}}^{\frac{\tau}{2}} dl \int_0^{2\pi} \int_0^{\alpha_{moon}} G'(\theta', \phi') sin\theta' d\theta' d\phi'$$

With the lunar solid angle calculated at each scan position, a linear regression model can be established to relate the calibrated lunar antenna temperature with the calculated antenna paramters as follow: For the *ith* lunar observation sample (where i=1,2,... n),

$$y_i = \alpha + \beta x_i + \epsilon_i$$

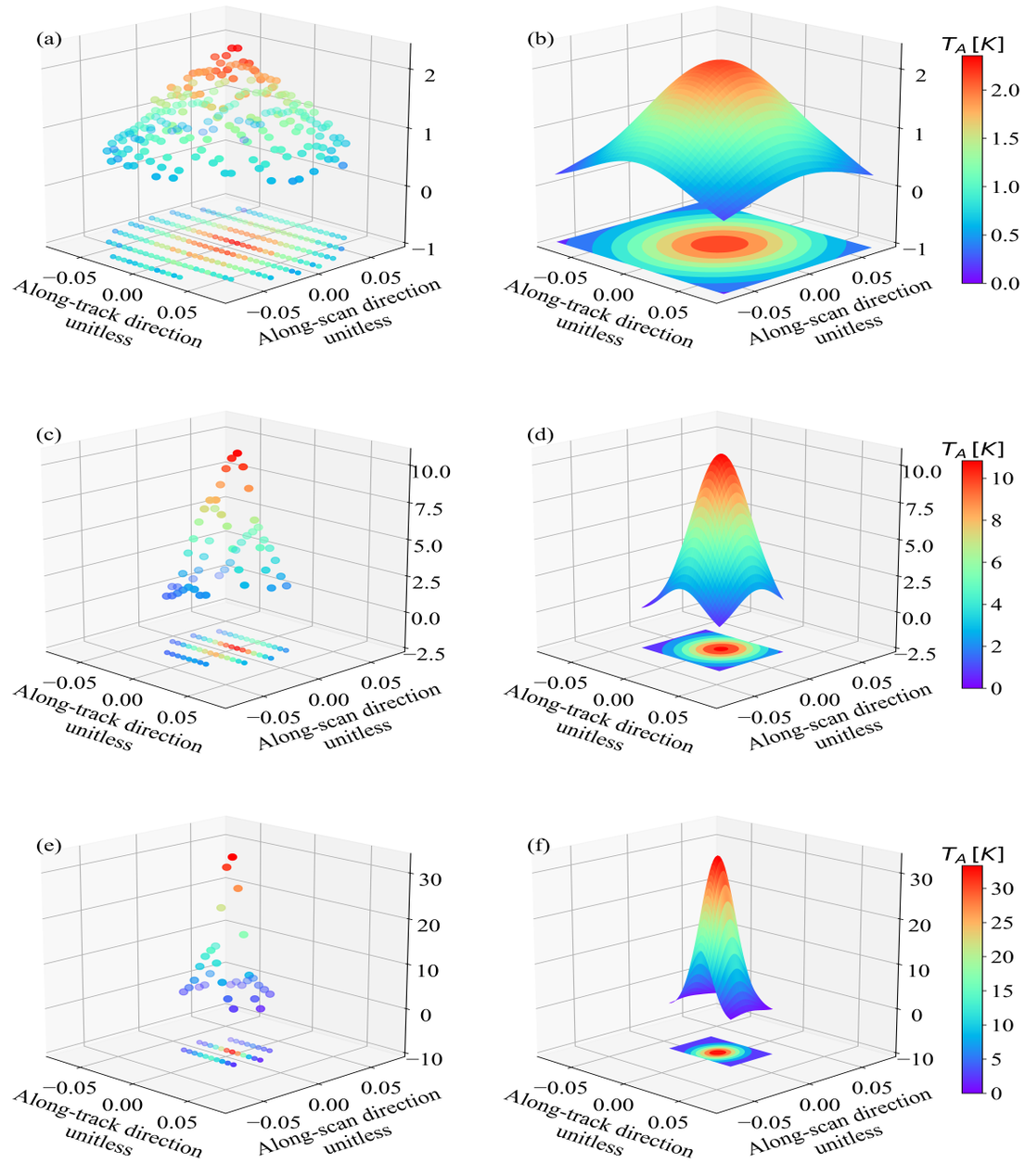

Results for Moon Disk-averaged Microwave Brightness Temperature Spectrum

*H. Yang et al., "2-D Lunar Microwave Radiance Observations From the NOAA-20 ATMS," in IEEE Geoscience and Remote Sensing Letters, doi: 10.1109/LGRS, **2020**, 3012518*

ATMS Ta spectrum of lunar's disk

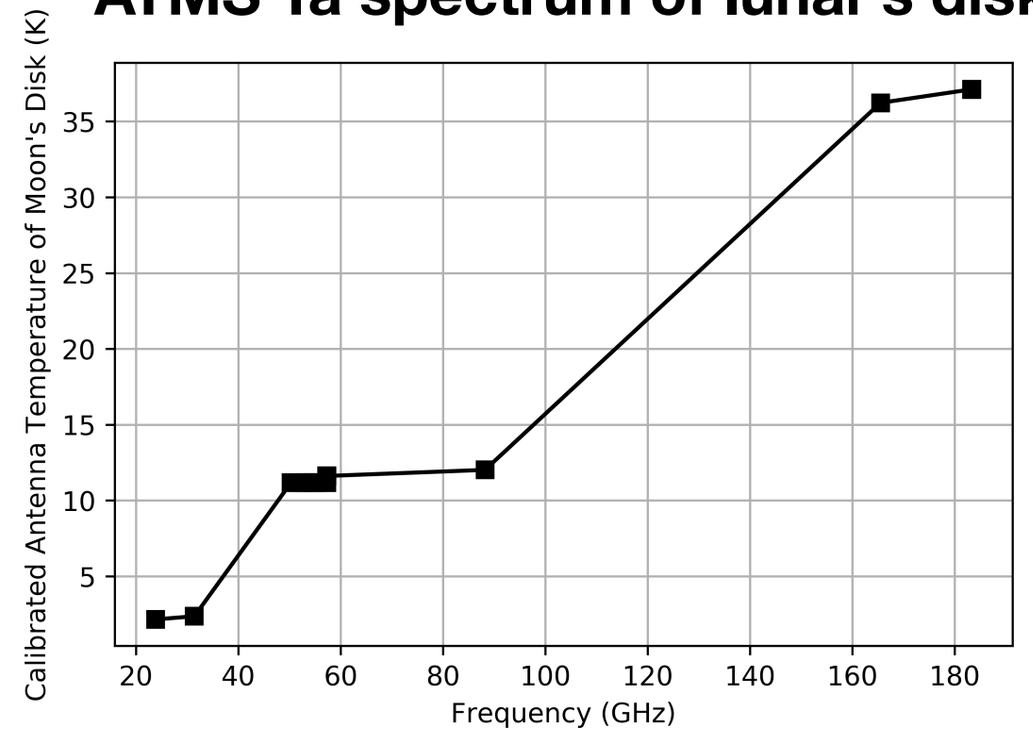

Antenna parameters and Calibrated Peak Antenna Temperature of the Moon

Band	Center Frequency (GHz)	Ω_P	Ω_{moon}^{Max}	Ta_{moon}^{Max}(K)
K	23.8	32.98	0.23	2.1
Ka	31.4	33.32	0.23	2.4
V	50.3–57	5.68	0.21	11.3
W	88.2	5.22	0.21	12.7
G1	165.5	1.54	0.16	33.0
G2	183.31	1.52	0.16	33.8

Tb spectrum of lunar's disk

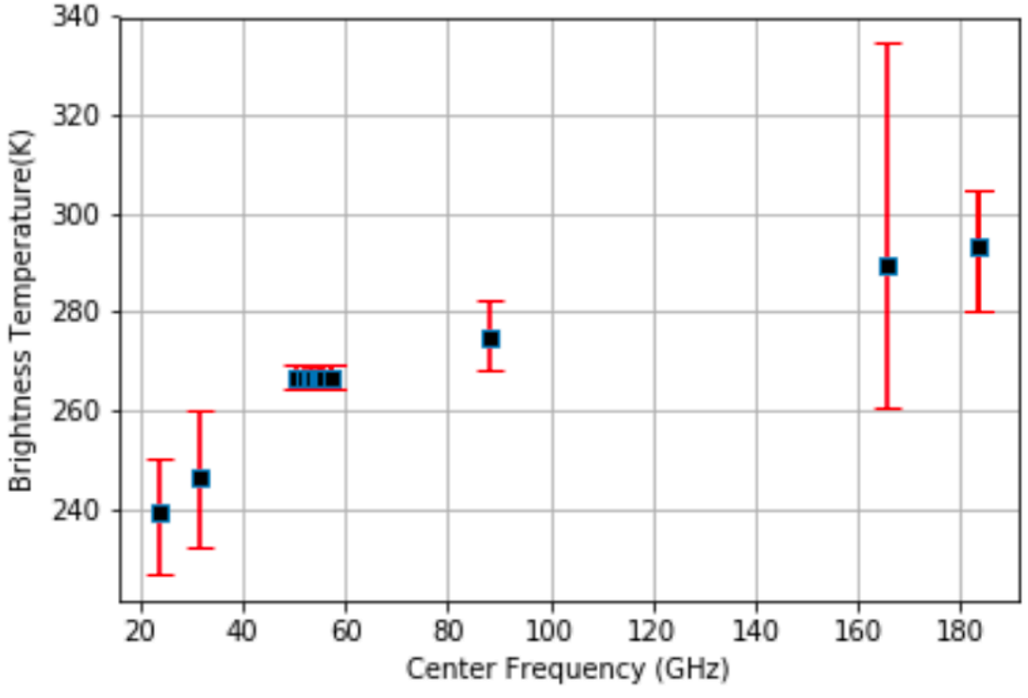

Retrieved Disk-integrated Tbs

Band	Center Frequency (GHz)	Tb_{moon}^{Disk} (K)	Lower Boundary of 90% Confident	Upper Boundary of 90% Confident
K	23.8	239.1	224.2	253.4
Ka	31.4	246.2	229.5	262.2
V	50.3–57	266.7	263.9	269.6
W	88.2	274.7	267.1	284.0
G1	165.5	289.7	222.7	336.3
G2	183.31	293.1	277.2	306.1

Moon Phase Angle Dependent Feature in Microwave Brightness Temperature of Moon's Surface

Moon surface temperature derived from the Diviner Lunar Radiometer Experiment instrument (DLRE) observations

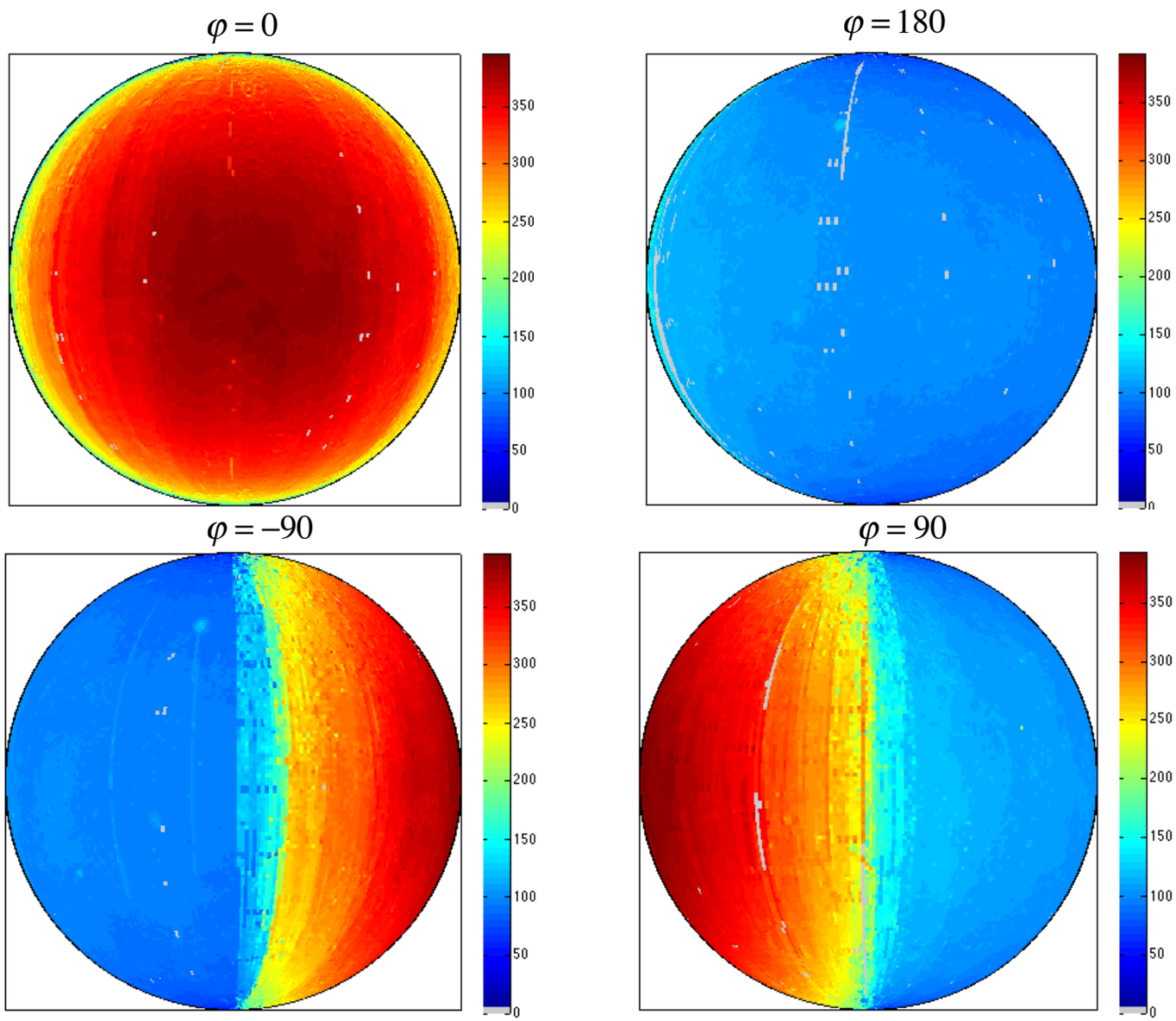

Moon Observations from AMSU Instrument on Drifting NOAA-18 Satellite

3D Projection of NOAA-18 Orbits from 2005 to 2019

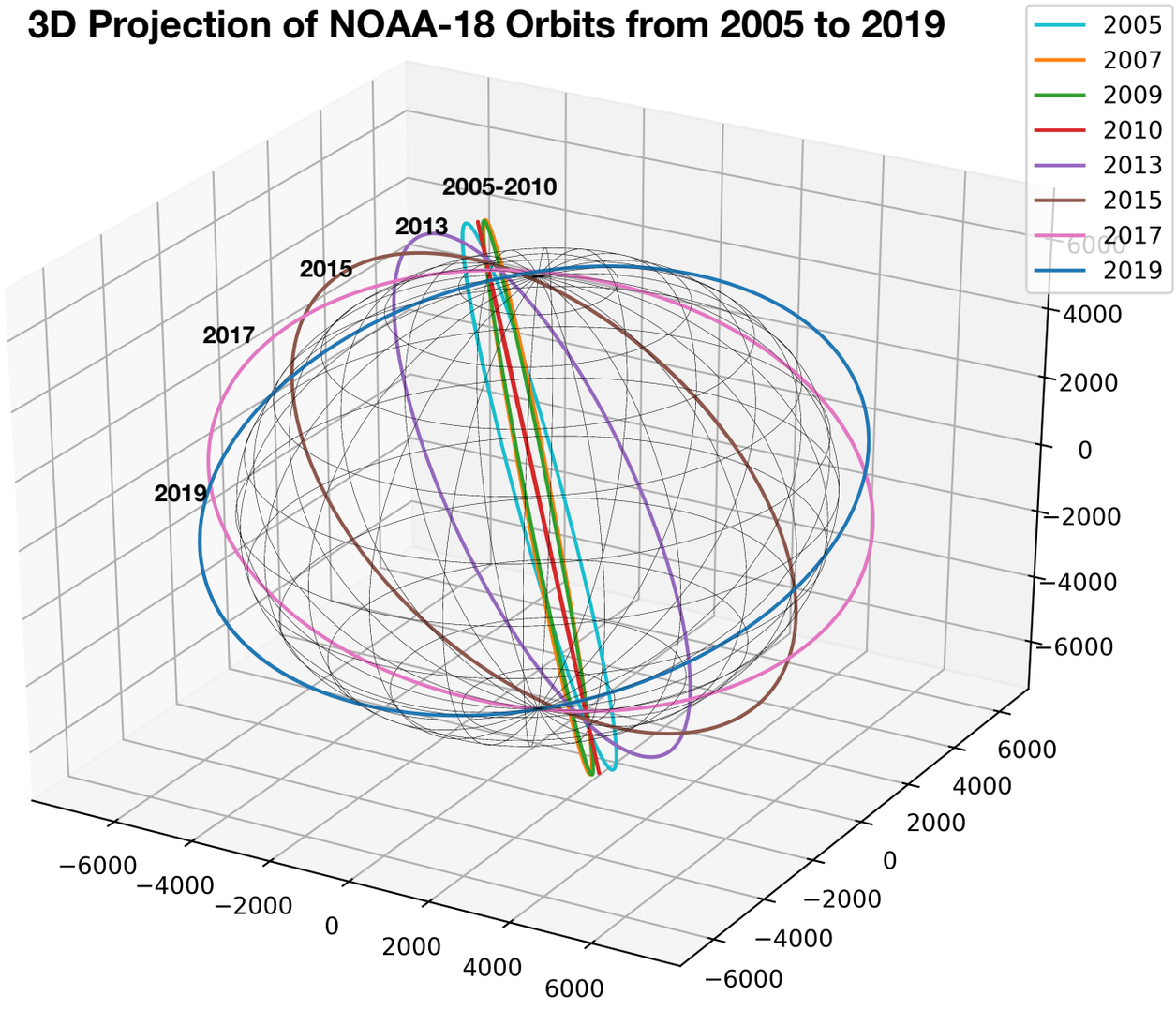

Change of Moon Phase Angle and LTAN of NOAA-18 Satellite

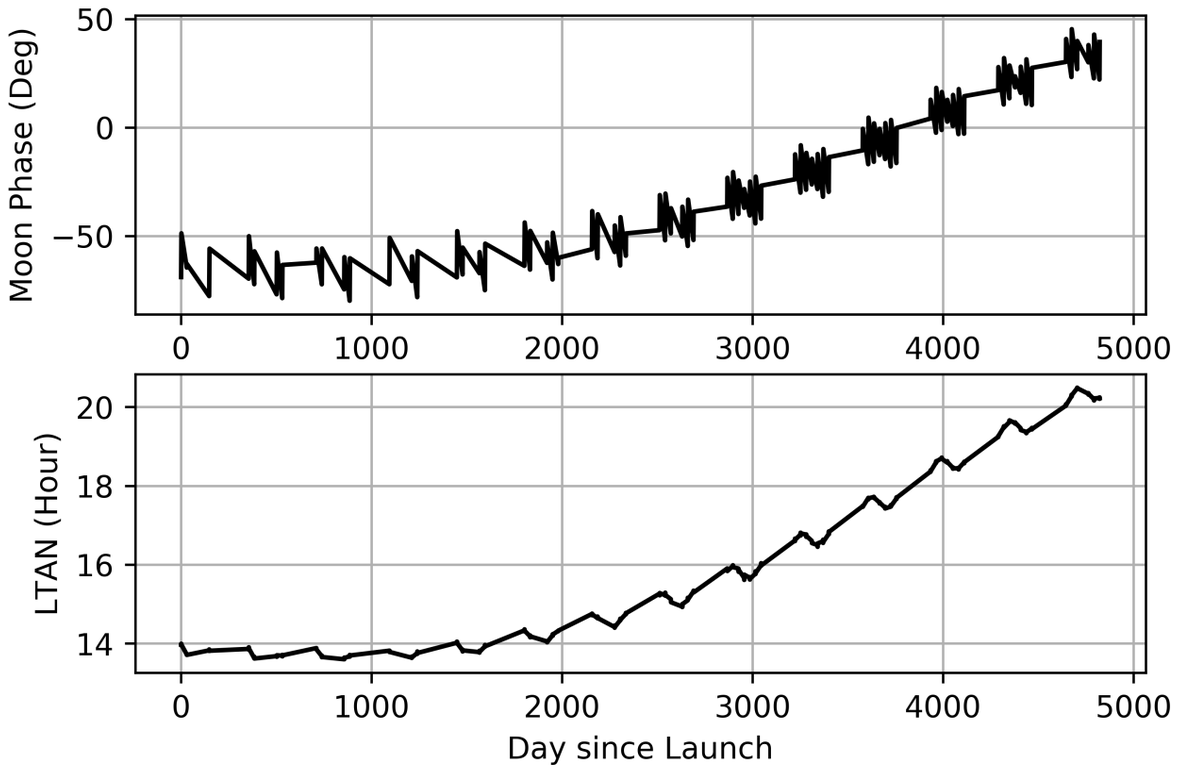

AMSU Lunar Intrusion Data Sampling and Calibration

AMSU LI samples can be identified from the position of Moon at the rotation antenna coordinate system. There is only one space view sample available at each scan of AMSU instrument, the searching for “clean” reference calibration counts is challenging since the calibration gain is keep changing during the LI process. LI free “clean” space view closest to the LI samples was taken to be reference at the starting time, then a successive substitution method was applied to derive the reference calibration counts

AMSU Scan Geometry

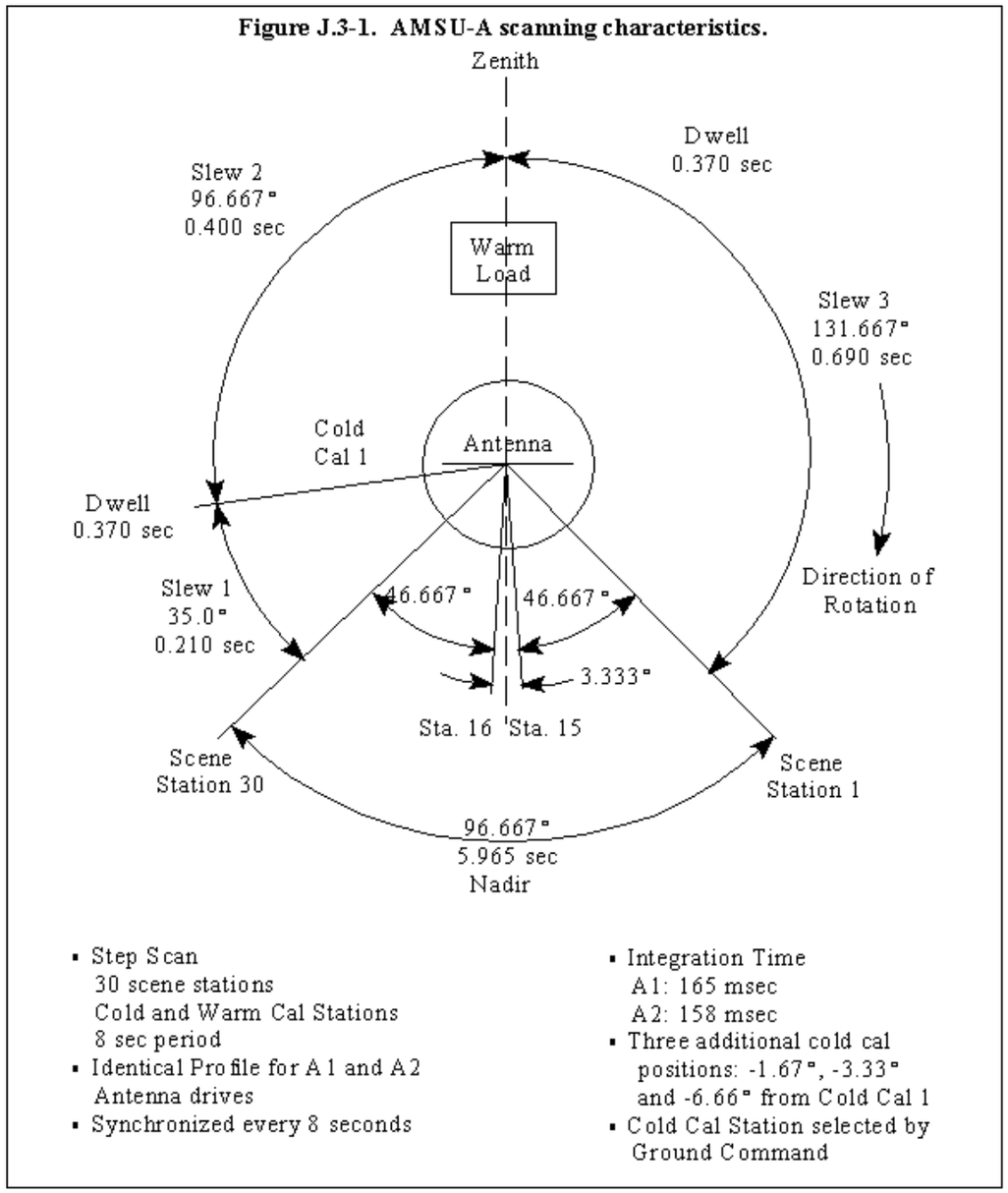

AMSU Channel 01 LI Samples

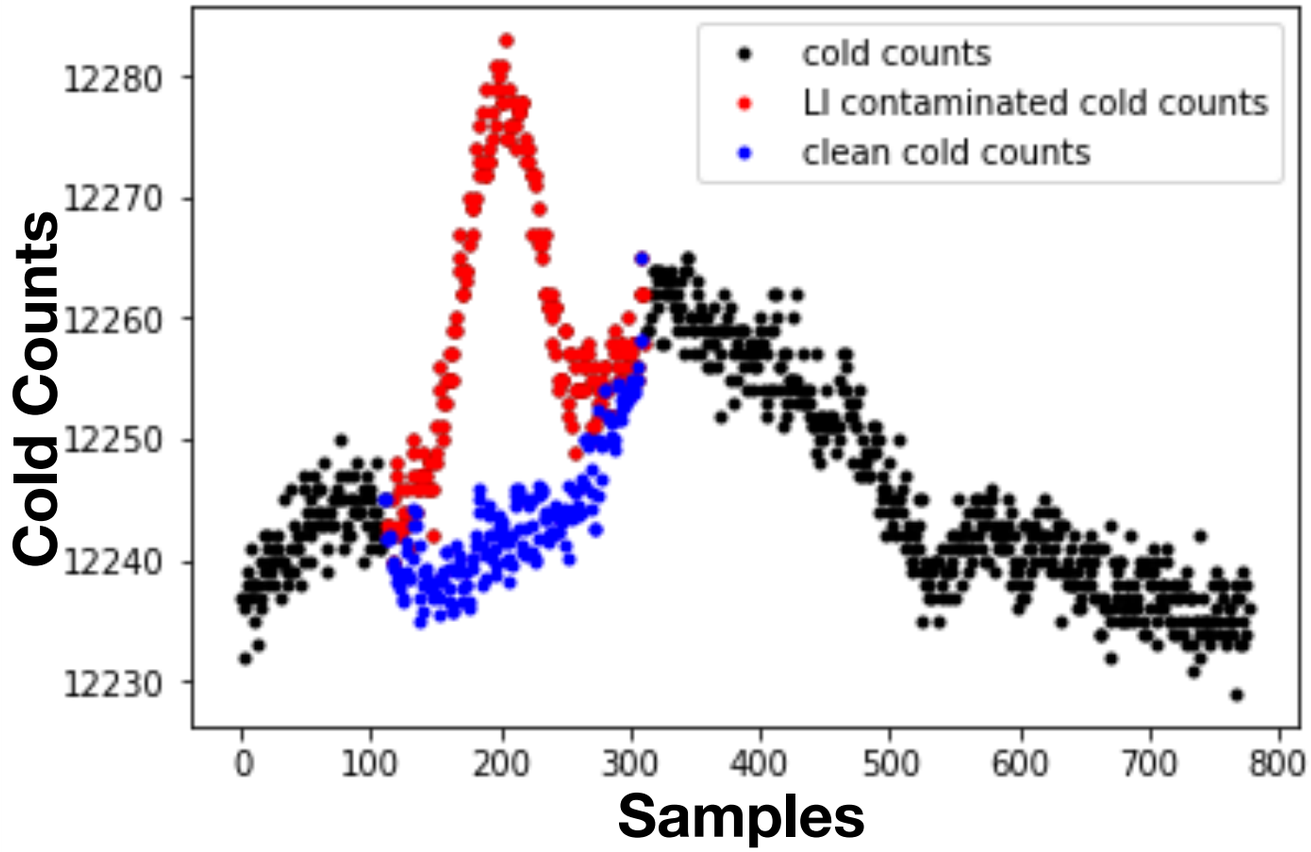

Calibration of lunar antenna temperature and Moon's disk integrated brightness temperature

Considering the fact that antenna pattern kept unchanged over the time, Moon brightness temperature spectrum at full moon phase from ATMS are used as anchor to derive AMSU antenna parameters. Tb at all other Moon phase angle can then be derived from the corrected antenna temperature

$$Ta_{moon} = G \cdot \Delta C_{moon} \qquad Tb_{moon} = \frac{Ta_{moon}}{\Omega_{moon}}$$

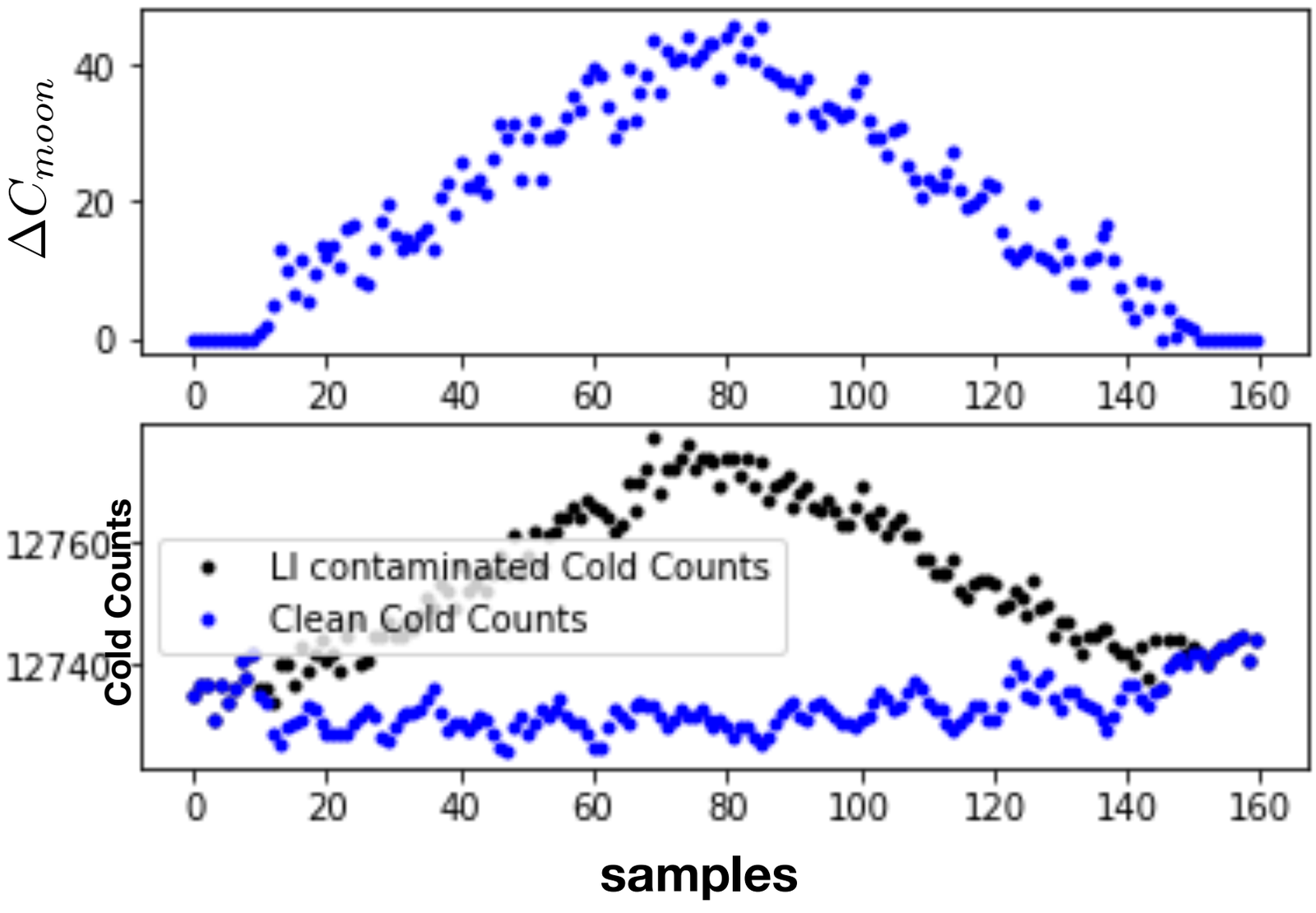

Moon Phase Angle Dependent Feature in Different Microwave Frequencies

***Yang, H.**; Burgdorf, M. "A Study of Lunar Microwave Radiation Based on Satellite Observations". Remote Sens. **2020**, 12, 1129*

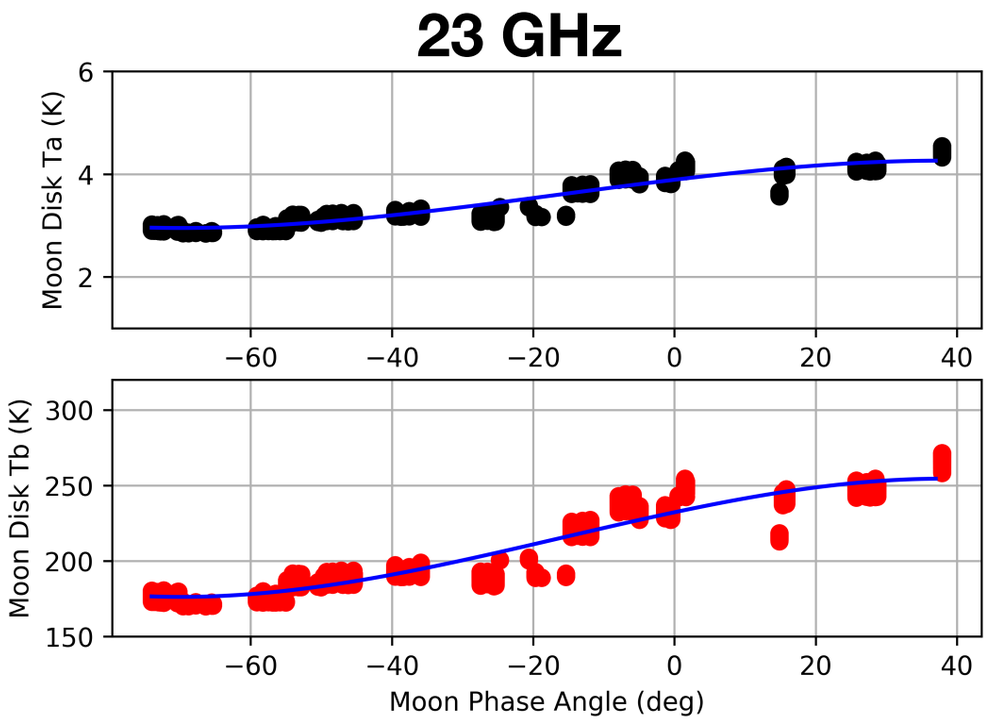

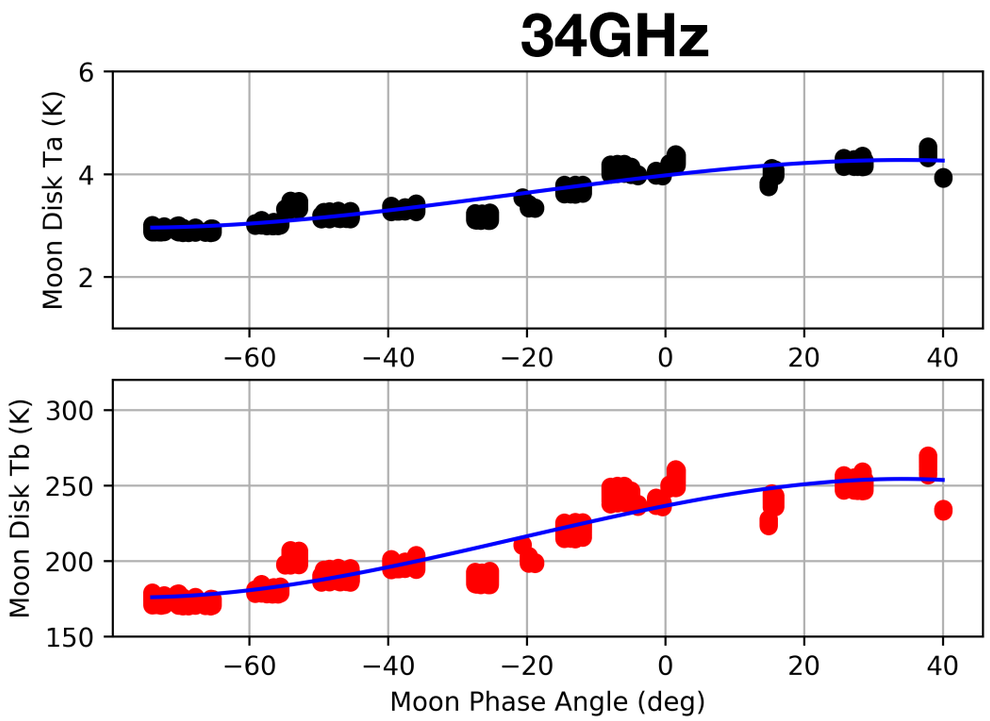

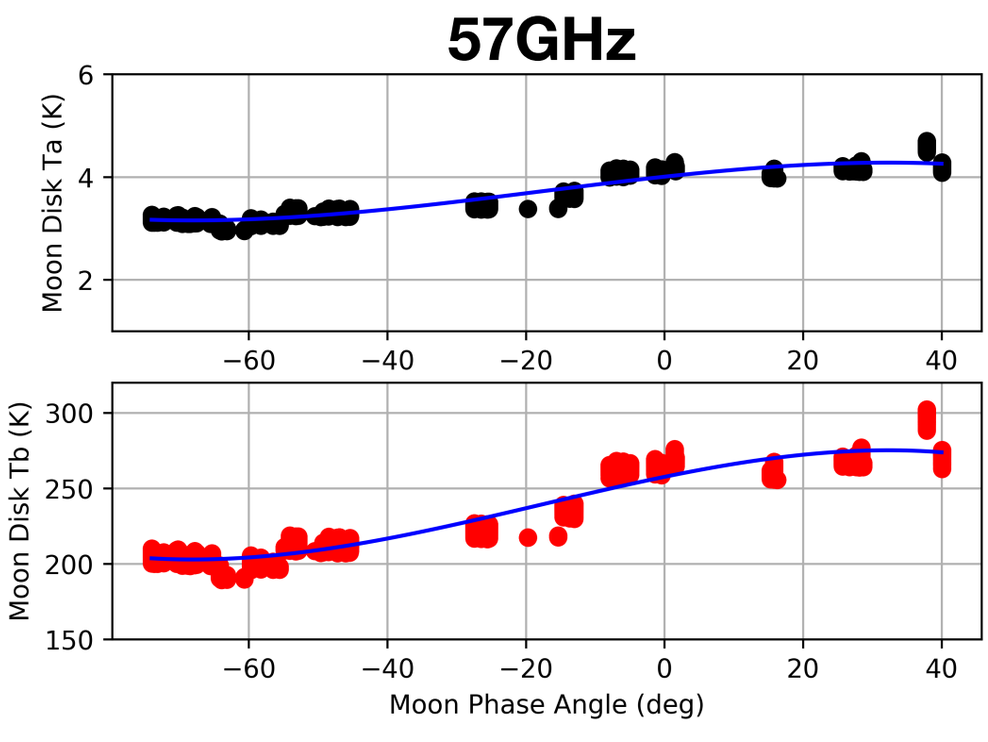

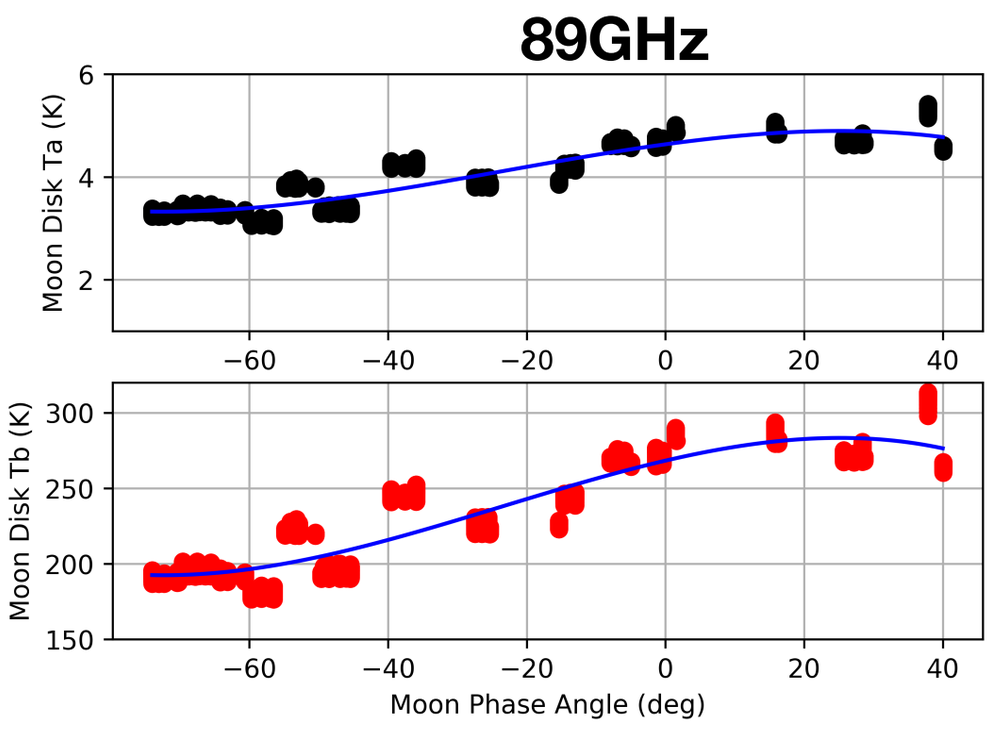

Theoretical Model for Microwave Emission of the Moon

(Stephen Keihm, ICARUS 60, 1984)

For a *purely absorptive* regolith, the correlation can be expressed simply as an integration of the depth-dependent emission, attenuated by the electrical loss to the surface. For a nadir observation,

$$TB(\lambda) = E_\lambda \int_0^\infty K_\lambda \cdot T(z) \cdot \exp\left[- \int_0^z K_\lambda dz' \right] dz$$

Lunar Surface Structure

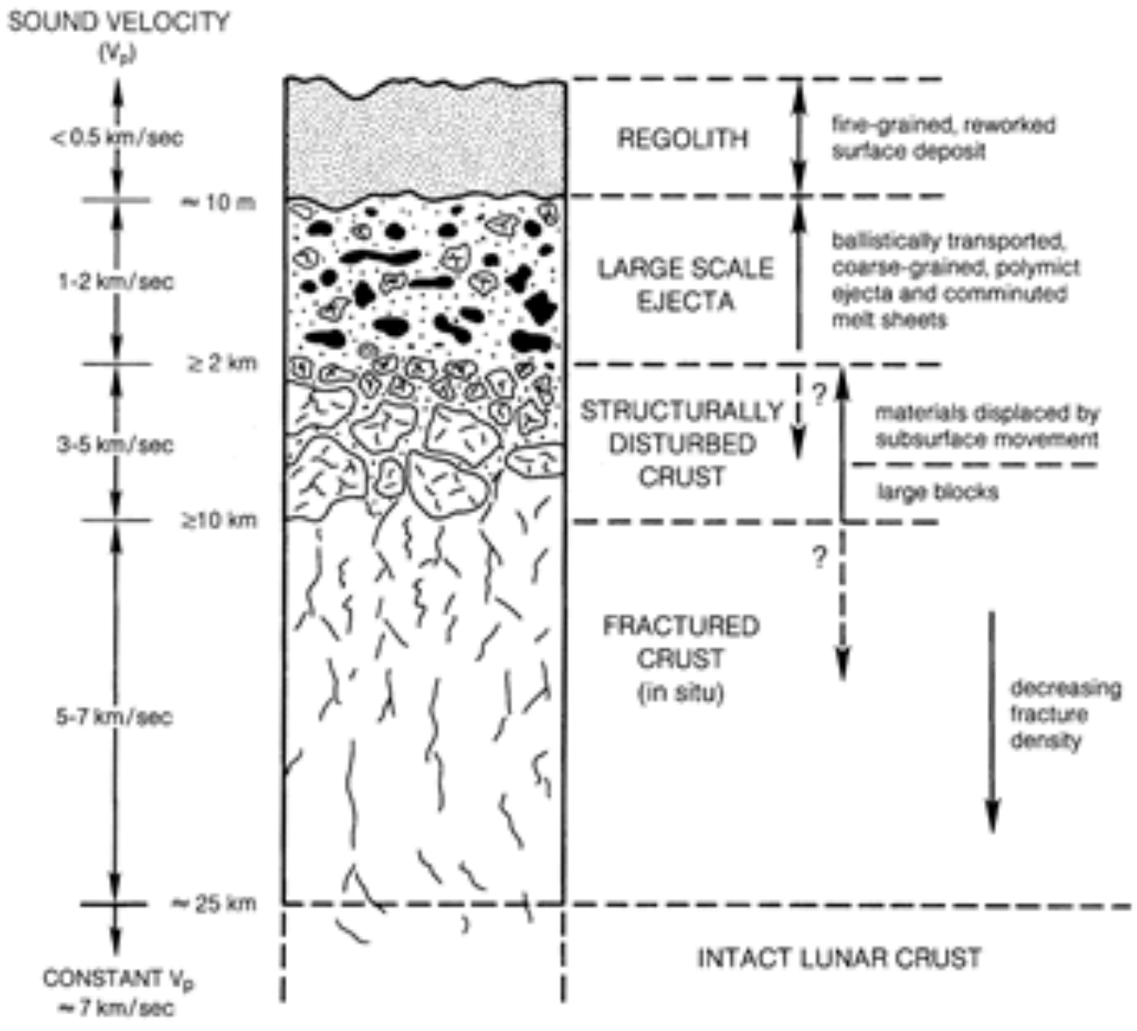

Heiken, G.H., Vaniman, D.T., & French, B.M. eds, **Lunar Sourcebook**, Lunar and Planetary Institute, Houston, 1991.

Temperature Profile of Lunar Regolith

Paul O.Hayne et al., "Global regolith therm-physical properties of the moon from the diviner lunar radiometer experiment", JGR Planets, 2017

Diurnal variation of T

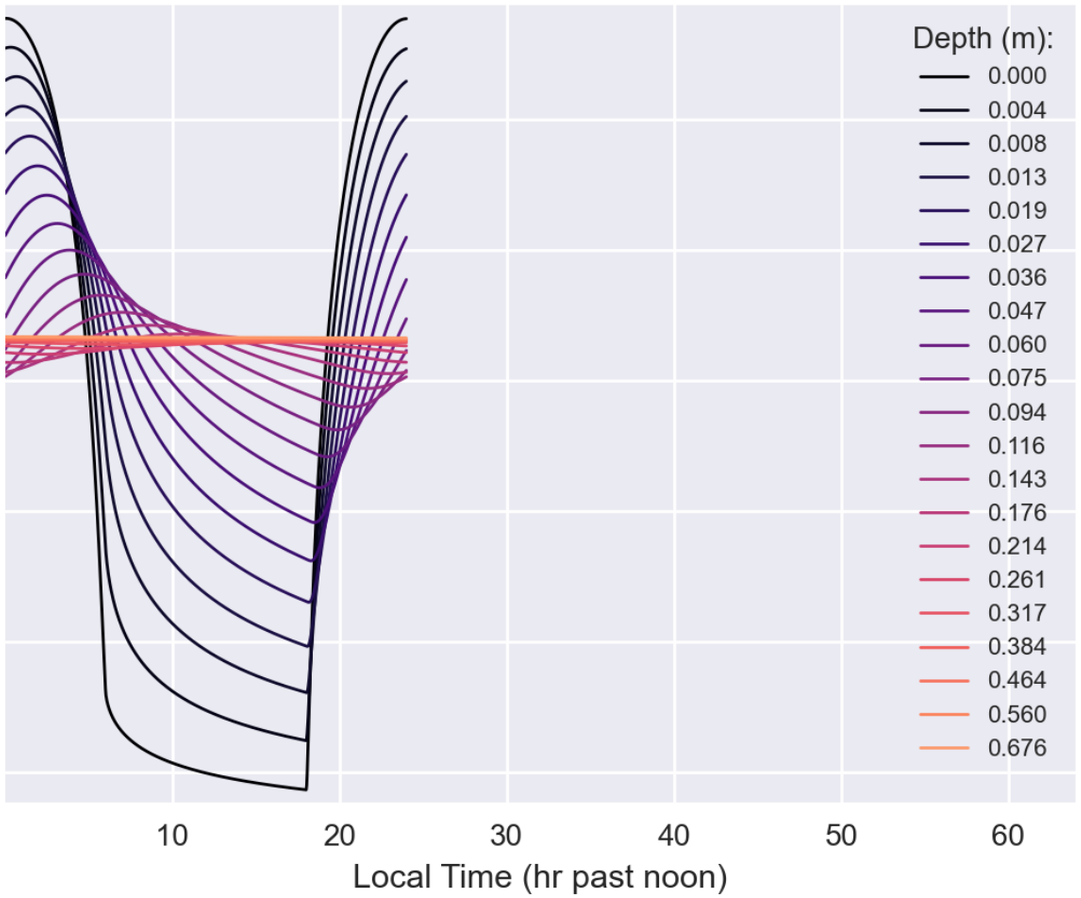

Profile of T up to 1 meter under Lunar Surface

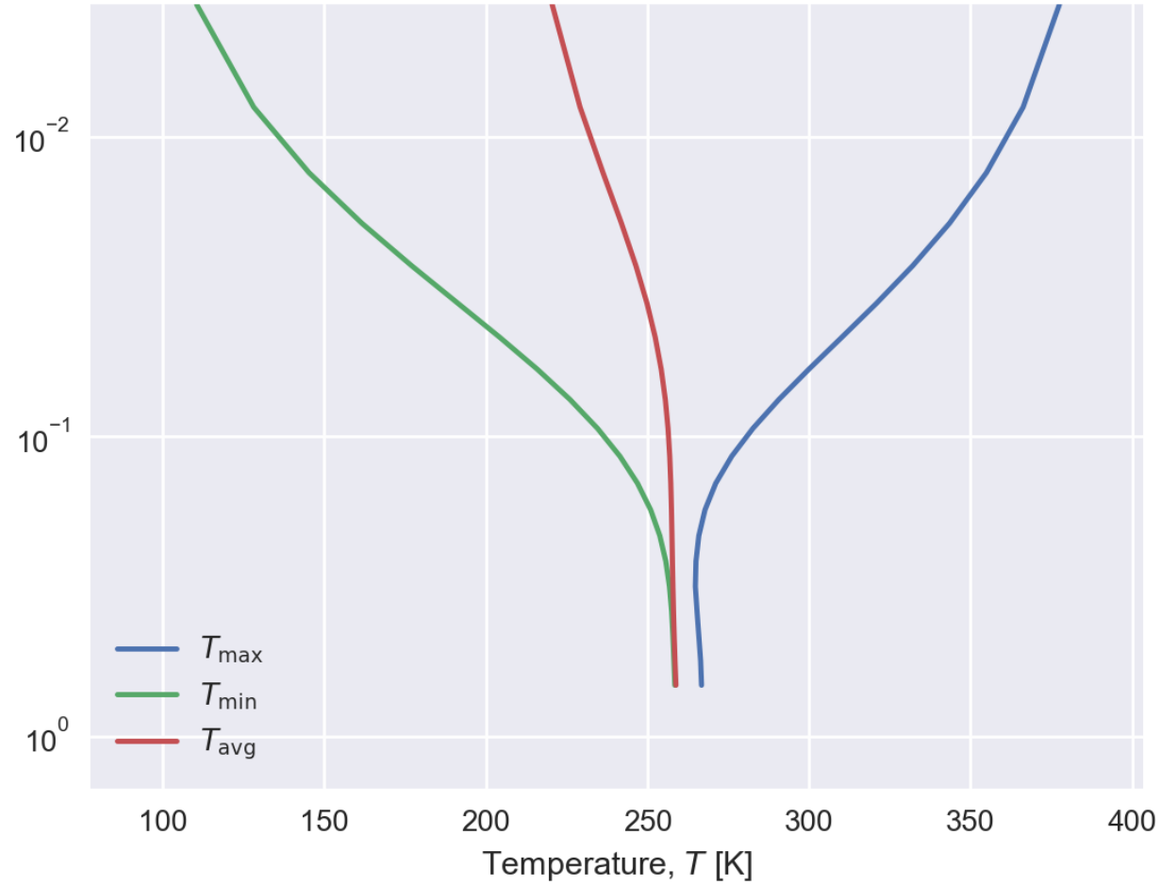

ICARUS 60, 568–589 (1984)

Interpretation of the Lunar Microwave Brightness Temperature Spectrum: Feasibility of Orbital Heat Flow Mapping

STEPHEN J. KEIHM

Planetary Science Institute, Science Applications, 2030 E. Speedway, Suite 201, Tucson, Arizona 85719

Received March 30, 1983; revised July 24, 1984

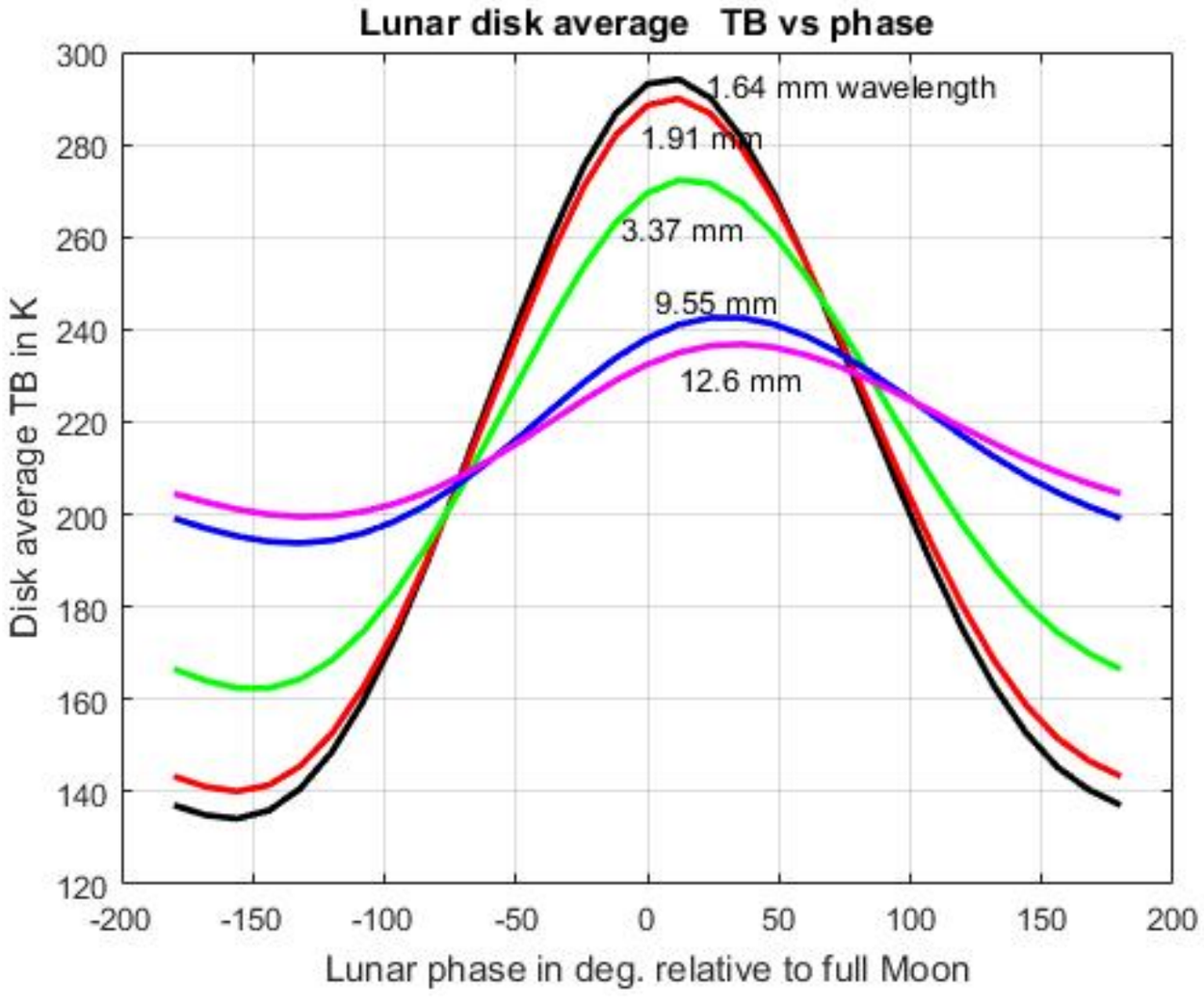

Potential of Taking Lunar Radiation as Cold End Calibration Reference for Instrument Across the Different Satellite Platform

- Radiance used in cold end is not clean cosmic background radiation, it includes contributions from other radiation sources such as Earth radiation from antenna sidelobe, thermal emission from reflector itself, as well as the thermal emission/reflection of satellite platform. The uncertainty of cold end radiance is different for each instrument and satellite platform, and is considered to be the major error source in TDR calibration.
- Lunar radiation is stable and highly predictable, and the lunar counts depends only on lunar radiance and instrument calibration gain. Therefore if a high accurate lunar radiance model can be established, the cold calibration radiance can be accurately determined by taking lunar radiance as reference.
- An absolute reference in cold end can not only improve the calibration accuracy, but also can reduce the inconsistency across the different satellite platform and therefore benefit for the development of CDR products

Sketch Plot of TDR Calibration

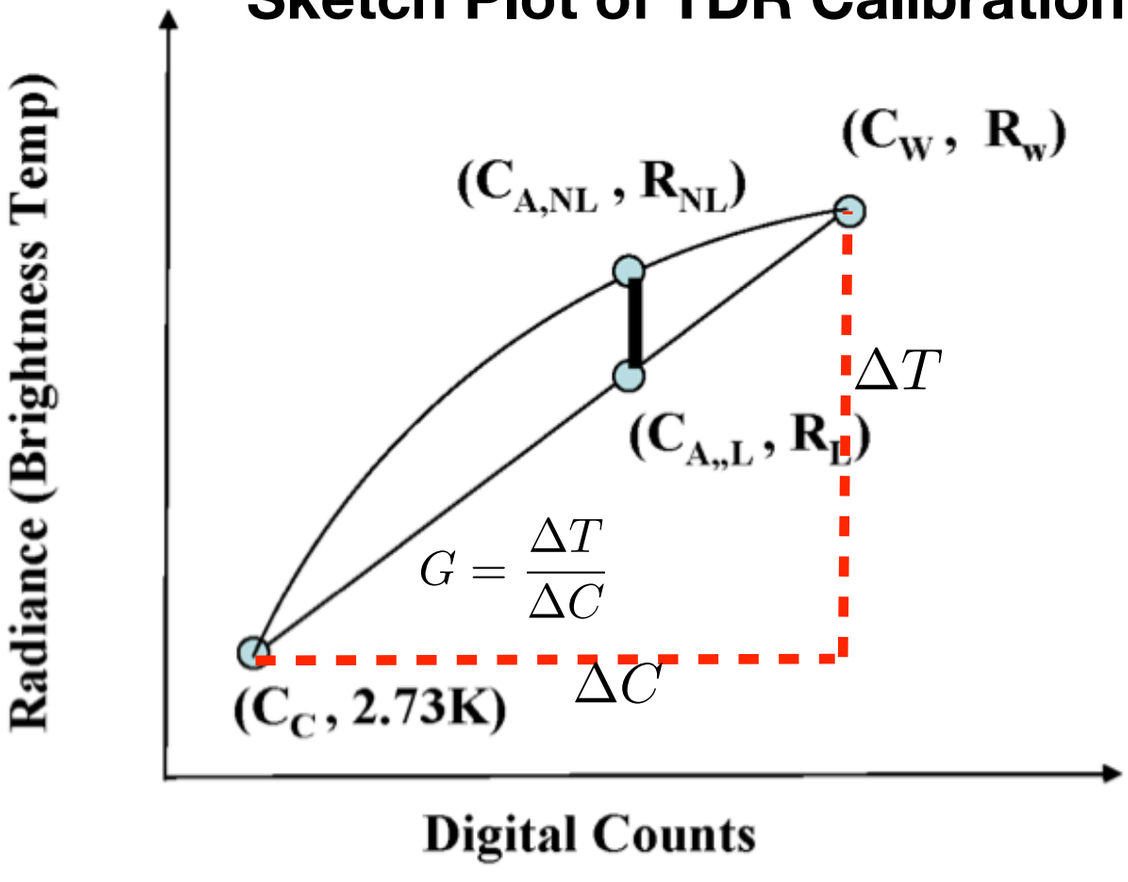

Lunar Calibration

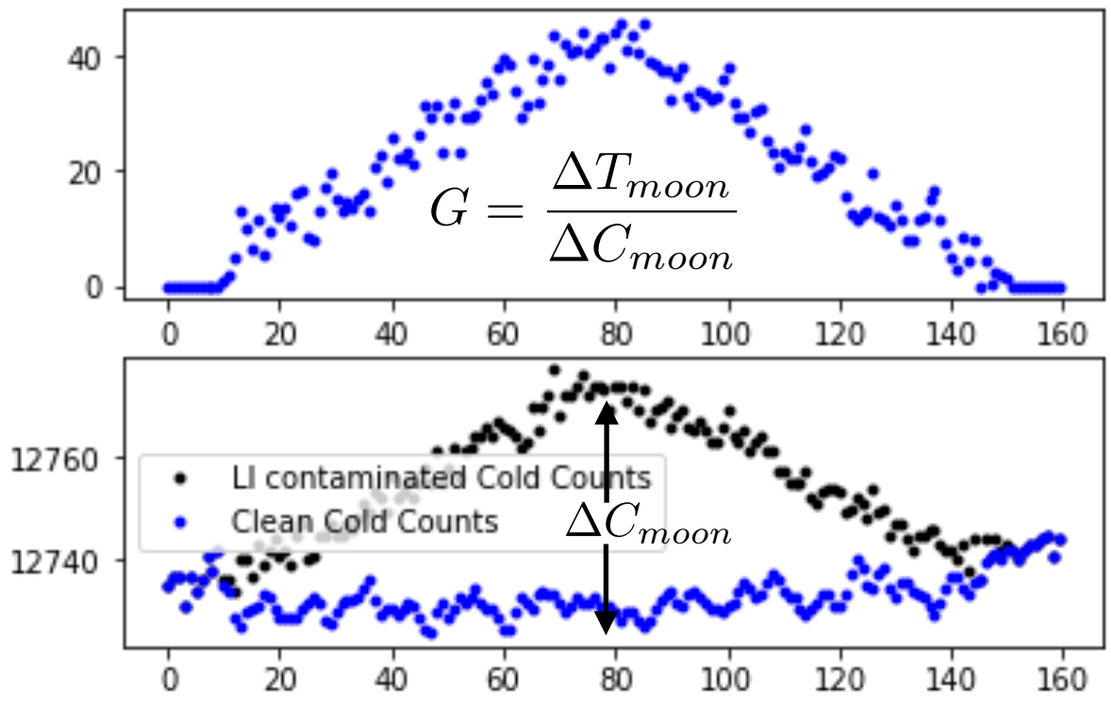

Vicarious Calibration by Taking Moon as Reference

Hu Yang, Jun Zhou, Ninghai Sun, Kent Anderson, Quanhua Liu, Ed Kim, 2018, "Developing vicarious calibration for microwave sounding instruments using lunar radiation", IEEE Transactions on Geoscience and Remote Sensing, Vol.99, PP.1-11

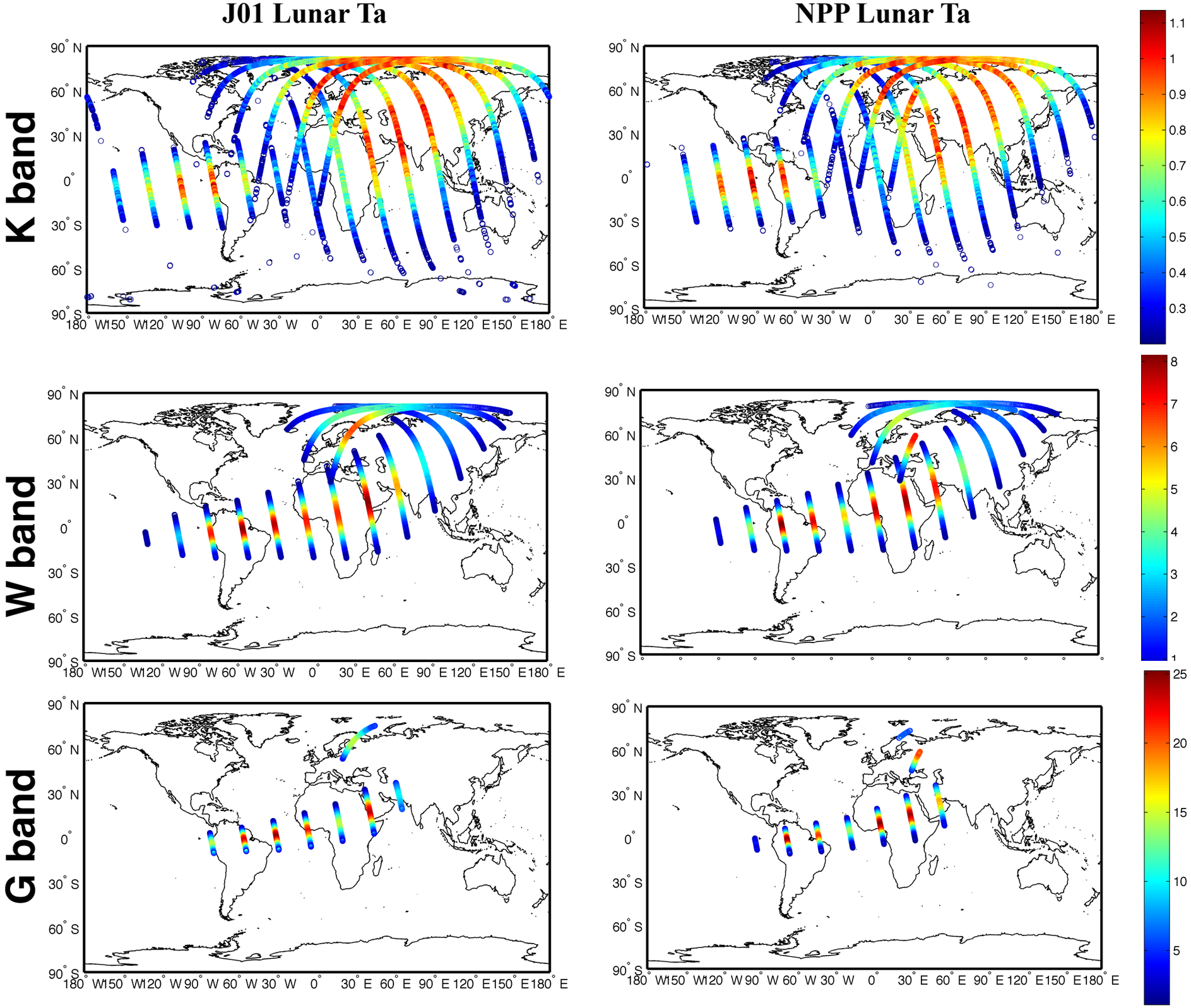

Long-term Instrument Stability Monitoring

Lunar as a Permanent Reference Target can also help to evaluate the long-term calibration stability of microwave sensors. Here, the lunar brightness temperature model developed in this work is used to simulate the effective brightness temperature of moon's disk, and then compared with the measurements from ATMS instrument. Sensor calibration stability can then be evaluated as

$$S = d(\Delta T_{moon})/dt$$

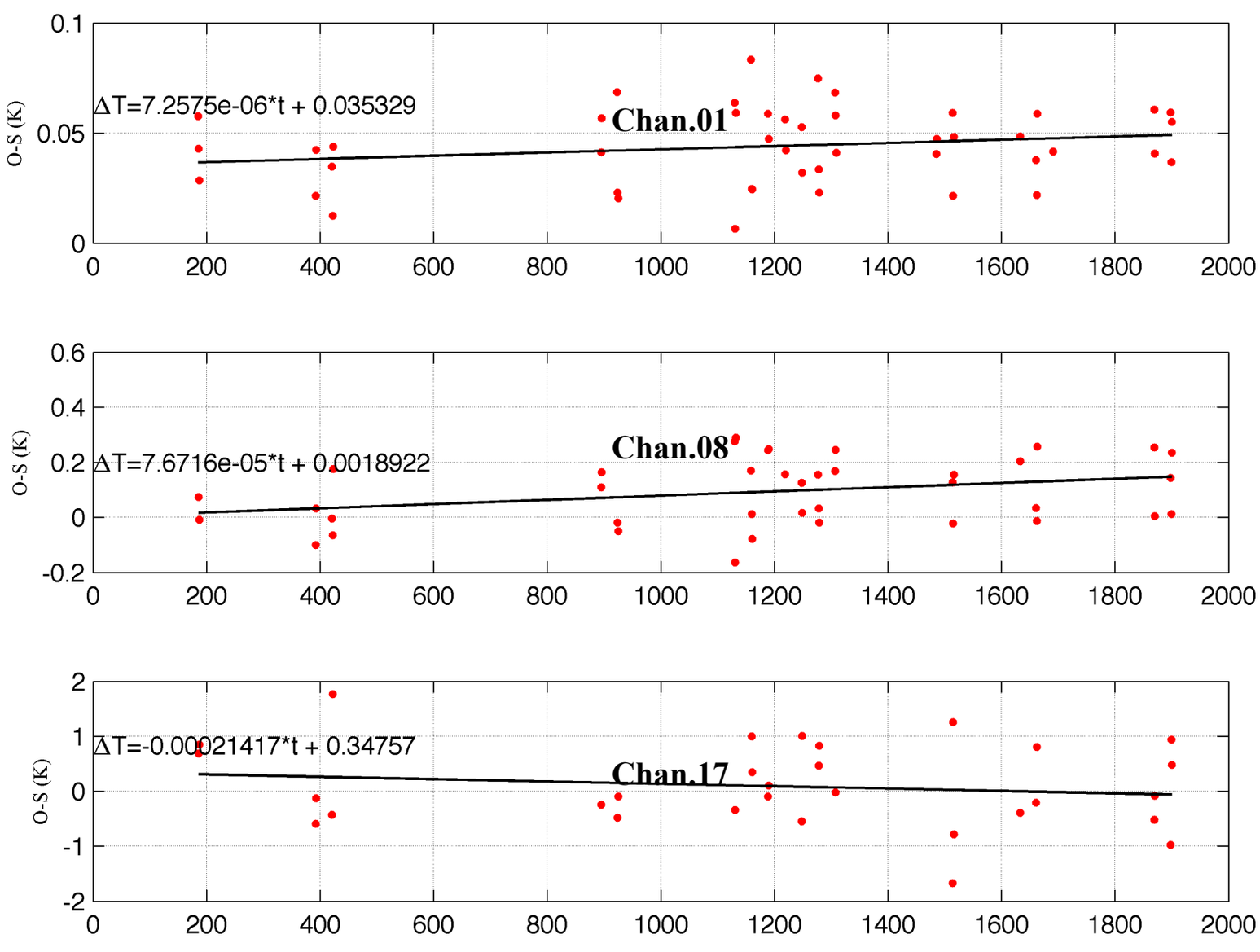

Conclusions and Future Work

- Lunar radiation is highly stable in microwave band and can be taken as permanent calibration reference target for microwave radiometers

- 2-D lunar scan observations from NOAA-20 ATMS and the lunar observations from drifting NOAA-18 AMSU provide a unique opportunity to obtain knowledge of lunar microwave brightness spectrum and phase lag in different frequency

- Future work is to build up a more comprehensive microwave emission model for Moon's surface by combing satellite observations and model simulations.